AD-A093 167 CAMBRIDGE UNIV (ENGLAND) DEPT OF ENGINEERING F/G 11/4
HYGROTHERMAL AGING EFFECTS ON THE MICROMECHANISMS OF CRACK EXTE--ETC(U)
1980 P D ANSTICE, P W BEAUMONT AFOSR-78-3644
UNCLASSIFIED CUED/C-MAT/TR.75-1980 AFOSR-TR-80-1244 NL

END
DATE FILMED
1 83
DTIC

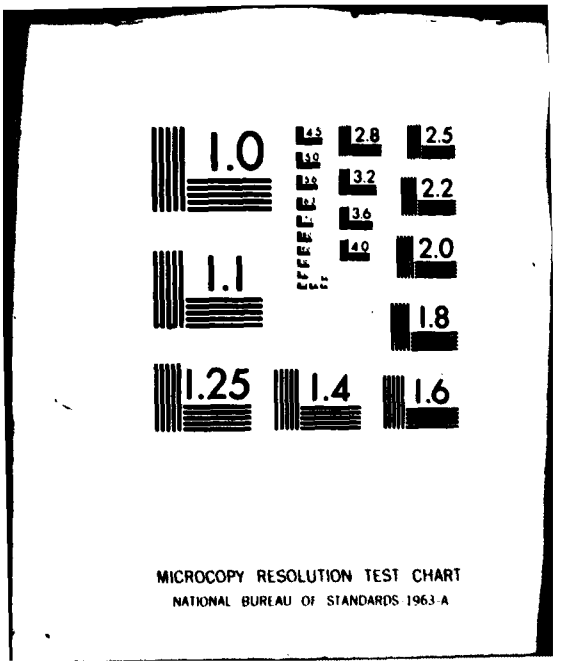
1.0
1.1
1.25
1.4
1.6
1.8
2.0
2.2
2.5
2.8
3.2
3.6
4.0
MICROCOPY RESOLUTION TEST CHART
NATIONAL BUREAU OF STANDARDS 1963-A

AFOSR-TR- 80-1244

(6)

LEVEL II

AD A093167

AFOSR-78-3644
FINAL

HYGROTHERMAL EFFECTS ON THE MICROMECHANISMS OF CRACK EXTENSION IN GLASS FIBRE AND CARBON FIBRE COMPOSITES

by

P.D. ANSTICE and P.W.R. BEAUMONT

CUED/C-MATS/TR.72 (1980)

DTIC ELECTE DEC 12 1980 S D C

DDC FILE COPY.

80 12 09 003

HYGROTHERMAL AGING EFFECTS ON THE MICROMECHANISMS OF CRACK EXTENSION IN GLASS FIBRE AND CARBON FIBRE COMPOSITES

Paul D. Anstice and Peter W.R. Beaumont

Department of Engineering, University of Cambridge,
Trumpington Street, Cambridge, England.

ABSTRACT

Hygrothermal aging effects and the micromechanisms of crack extension in glass fibre and carbon fibre composites are described. A new collection of failure data based on direct observation of fibres debonding, breaking and pulling out of a cracked epoxy matrix is presented. The data are summarised in cumulative probability diagrams which provide a convenient means for the comparison of fracture behaviour of composite systems. These diagrams also demonstrate the effects of changes in environment and time in a given experiment in a manner useful for the failure analysis of a fibrous composite.

KEYWORDS

Micromechanisms of fracture; glass fibres; carbon fibres; hygrothermal effects; failure analysis; probability of failure.

INTRODUCTION

Many brittle solids, glass and epoxy resin are examples, may under a certain stress-state and environmental condition, exhibit stress corrosion cracking. The micromechanisms of crack extension in glass are well documented. Less well understood are the fracture-mechanisms of thermosetting resins. In brittle fibrous composites, glass fibres in epoxy, for instance, fracture involves additional microfracture processes, decohesion of the fibre-matrix interface, snapping of fibres at weak points, and the extraction of fibre ends from matrix sockets. We know from earlier work that the fracture of glass and epoxy is time-dependent and moisture-sensitive. It is logical to assume, therefore, that the micromechanisms of crack extension in brittle fibrous composite systems, glass fibres and carbon fibres in epoxy, will also be sensitive to fluctuations in temperature and humidity, and time in a given experiment.

This paper describes a study of the failure of glass fibres and carbon fibres in epoxy, and the effects of hygrothermal aging. A knowledge of the fracture-mechanisms in monotonic loading is important because they are the origins of a material property which we call *toughness*. The study involves the observation of microfracture events; the measurement of toughness as a function of humidity and aging

time; and the identification of the principle methods of toughening. To do this, we use a model fibrous composite (Kirk, Munro and Beaumont, 1978) to evaluate the work of fracture or toughness and permit the direct observation of modes of failure. An optical microscopic technique is used to measure the distance over which fibres separate or debond from the matrix, and later pull-out after breaking at weak flaws. We construct diagrams of cumulative probability which display a vast amount of failure data collected from a large number of measurements of debonded and pulled out fibres. The effects of hygrothermal aging become clear from comparisons of these diagrams. Finally, we use previously derived equations (Harris, Morley and Phillips, 1975) (Kirk, Munro and Beaumont, 1978), based on physically sound models of fracture, together with the failure data to estimate the work to fracture the composite. A comparison between the experimental work of fracture measurement and predicted value of the total energy dissipated helps to distinguish the micromechanisms of fracture and the hygrothermal effects of aging.

EXPERIMENTAL

The model composite consists of a rectangular beam of epoxy resin and a single layer of 5 glass fibre rovings or 5 carbon fibre tows embedded in the resin (Kirk, Munro and Beaumont, 1978). Each roving or tow contains 1600 glass filaments or 5000 carbon filaments, respectively. The specimen has about 1.5 mm of resin on one side of the fibres and 0.5 mm on the other and resembles a single ply of a laminate. A shallow groove runs along the mid-point of the beam on the face closest to the fibres and perpendicular to the fibre direction. We use an epoxy resin supplied by Ciba-Geigy Limited designated LY567. It is made by mixing 100 parts of resin and 36 parts of hardener (HY567). The composite is cured at room temperature for 24 h and post-cured at 100°C for 16 h. Some of the samples are exposed to 95% relative humidity (RH) and 100°C for various lengths of time between 1 h and 4 weeks; other samples are aged at 100°C, 0% RH before testing.

Each specimen is loaded in 3-point bending using a displacement-rate of 3×10^{-2} mm/s and the fibres at the root of the notch on the tensile side of the beam fail in tension. The fibre-matrix interface fails at the root of the notch and a debonded zone spreads slowly under conditions of increasing load along the fibre (Munro and Beaumont, 1979). Both halves of the broken test-piece are viewed in an optical microscope and the distances over which the fibres have debonded and subsequently pulled-out after fracture can be measured.

The work of fracture or toughness is calculated by dividing the area under the load/deflexion curve by twice the total cross-sectional area of fibres. We ignore the small contribution made by the matrix to the toughness of the composite. In this way, a direct comparison between experimental work of fracture data and predicted fracture energy based on models of fibre debonding and fibre pull-out is possible.

STATISTICAL ANALYSIS OF FAILURE DATA

The analysis of failure data is based on the Weibull or extreme value distribution method which enables information to be presented in a useful form. This alternative way of using Weibull analysis is to relate the probability, P, of observing a fibre debonding or pulling out over a particular distance, ℓ;

$$P = 1 - \exp(-\ell/\ell_o)^m V \qquad (1)$$

ℓ_o is a reference fibre length; m is the Weibull constant; and V is the volume of the specimen, (for simplicity, we make V = 1). In logarithmic form

$$\ln(-\ln(1-P)) = m(\ln \ell - \ln \ell_o) \quad (2)$$

which predicts a linear relationship between $\ln(-\ln(1-P))$ and $\ln \ell$. m is the gradient of the plot and the intercept is $\ell = \ell_o$ when $P = e^{-1} = 0.37$. To construct the cumulative probability diagram we arrange serially j = 1,2, ...N values of fibre debond length and fibre pull-out length in increasing order of length. The probability is defined as

$$P = (j - 0.5)/N \quad (3)$$

where N is the number of observations. A characteristic value, $\bar{\ell}$, of a distribution of data in the form of eq. (1) can be expressed as (Beaumont and Anstice, 1980)

$$\bar{\ell} = \int_{\ell_1}^{\ell_n} (\ell \, dP/d\ell) \, d\ell \quad (4)$$

$$= \int_{\ell_1}^{\ell_n} m(\ell/\ell_o)^m \exp(-(\ell/\ell_o)^m) \, d\ell \quad (5)$$

WEIGHT CHANGES

Exposure to extremes of humidity at 100°C results in a change of weight (ΔW) with time (t), of epoxy, glass fibre-epoxy and carbon fibre-epoxy (Fig. 1). The initial slope of a weight versus $(\text{time})^{\frac{1}{2}}$ curve for matrix and composite aged at 95% RH is linear. It suggests that the diffusion of water is Fickian controlled, i.e., $\Delta W \propto t^{\frac{1}{2}}$. Complete saturation is achieved after 5 days, approximately, corresponding to a water content of about 3 $^{w}/_{o}$. In Fig. 1, data are normalised to the volume fraction of epoxy. The superposition of data indicates that the diffusion mechanism is in some way determined by the matrix.

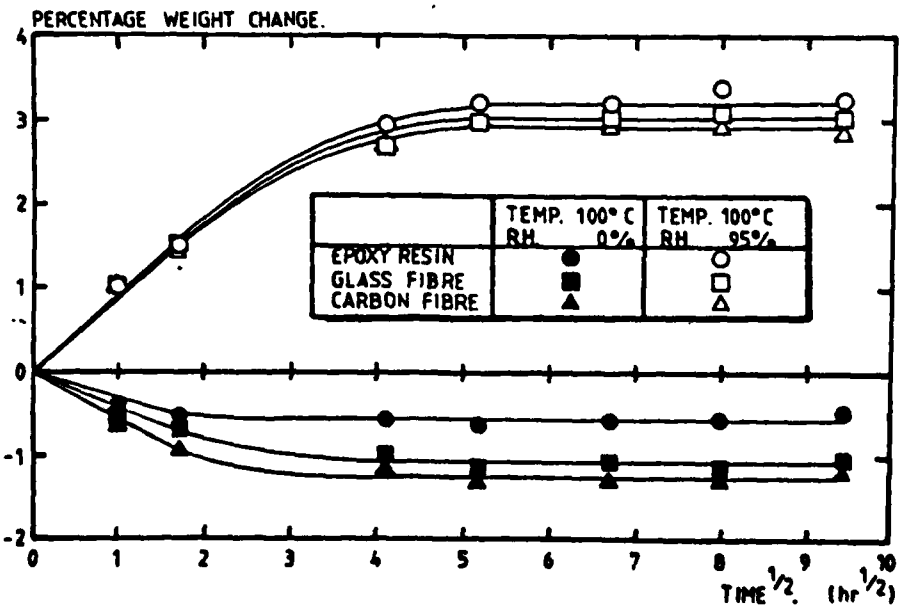

Fig. 1 Change of weight of resin and composite as a function of humidity and aging time.

In contrast, aging of epoxy and composite at 100°C, 0% RH results in a decrease in weight. We believe a loss of volatiles from the epoxy takes place. An additional weight loss of the composite may be due to drying out of the glass fibres and carbon fibres originating as moisture absorbed onto the surface of the fibre before impregnation with resin.

WORK OF FRACTURE

The work of fracture data for composites aged at 100°C, 0% RH are shown in Fig. 2. For glass fibres in epoxy, a precipitous fall in toughness by nearly one-half occurs after 1 h. This drop in toughness is almost recovered after 1 day but the toughness

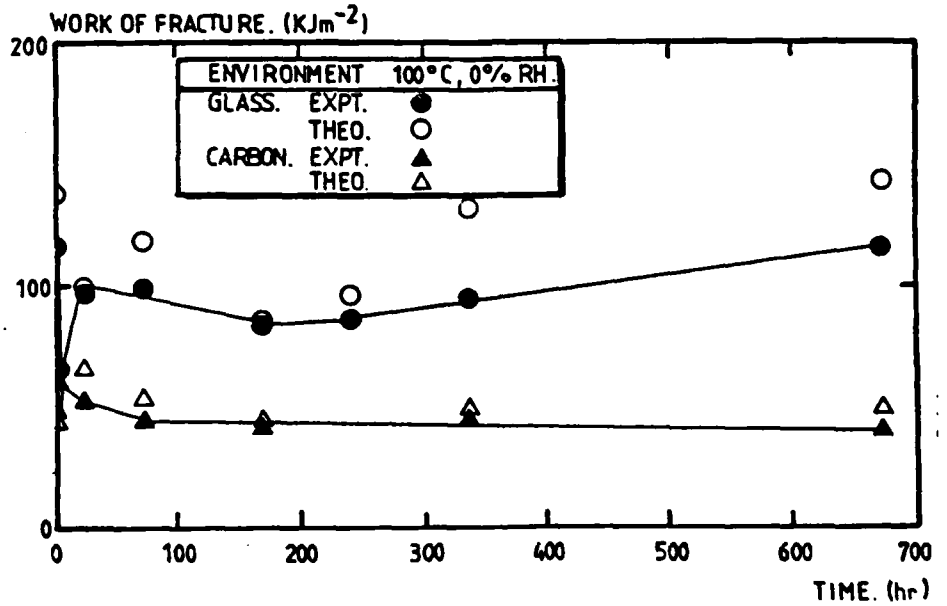

Fig. 2 Work of fracture of composite as a function of aging time (100°C, 0% RH)

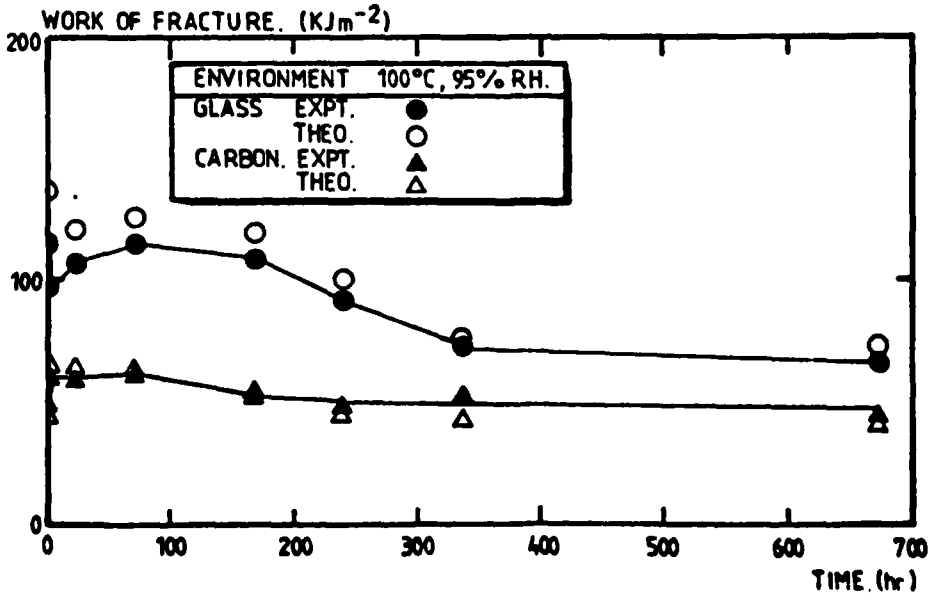

Fig. 3 Work of fracture of composite as a function of aging

lls again during the next 150 h or so. Aging for 1 week produces a minimum in work of fracture curve of ca. 80 kJ/m^2. Over the next 3 weeks or so, we see a eady rise in toughness towards the original value. For carbon fibres in epoxy, initial increase in work of fracture after 1 h is followed by a gradual decrease a constant value of ca. 40 kJ/m^2 after 100 h, approximately.

posure of glass fibre-epoxy to 100°C, 95% RH for 1 h causes the work of fracture fall by nearly one-fifth to ca. 95 kJ/m^2 (Fig. 3). The initial work of fracture recovered after 3 days before falling over the next 2 weeks to a value of ca. kJ/m^2. The data collected for carbon fibres in epoxy shows a trend similar to one observed during aging at 100°C, 0% RH.

CUMULATIVE PROBABILITY DIAGRAMS OF FAILURE DATA

ure data of fibre debond length and fibre pull-out length collected in the tographic analysis are presented in the following cumulative probability diams (Figs. 4-9). In Fig. 4 are shown data of debond length of glass fibres in xy after aging at 100°C, 0% RH. Each distribution of data do not superimpose are displaced relative to one another. Inspection of positions of sets of ilure data reflect the observed variations in shape of the experimental work of acture curve. For example, specimens tested after manufacture (t = 0) produce ilure data which fall towards the right of the probability diagram, or have high lues of fibre debond length. Failure data collected after 1 h are on the left of diagram and correspond to low values of debond length. Each subtle movement of set of data to higher and lower values of debond length for aging times between h and 28 days correlate with a rise and fall of the curve drawn through the asurements of work of fracture. The Weibull constant m describes the spread of ilure data for each aging cycle (Table 1). For an aging time of 10 days m = 3, d between 2 and 4 weeks m = 2, approximately. The difference may not be signifint, but when considered together with the shift of failure data with time, a hange in m may suggest a variation in mechanism of fracture.

The distribution of failure data to describe the extraction of broken glass fibre ends is shown in Fig. 5. The data fall in a narrow band with superposition at low probabilities and low values of fibre pull-out length, with slightly displaced data at P = 1. In general, a slight variation in shape and position of a probability curve reflects the observed changes in work of fracture with time. For t = 1 h, failure data lie close to the left of the band. After 1 day, the distribution has

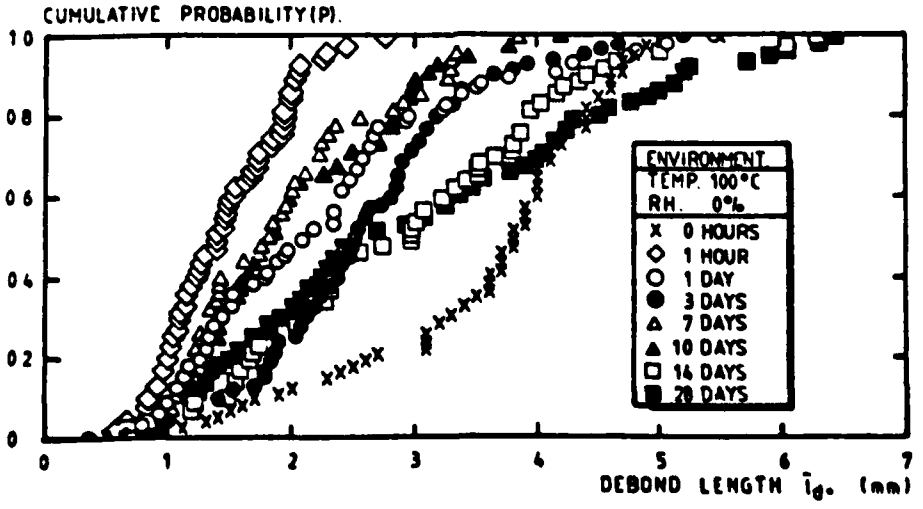

Fig. 4 Distribution of glass fibre debond lengths for various

TABLE 1 Values of the Weibull constant m for the debonding and pulling out of glass fibres and the pulling out of carbon fibres in epoxy

	Debonding glass	Pull-out glass	Pull-out carbon	Debonding glass	Pull-out glass	Pull-out carbon
n)	(100°C , 0% RH)			(100°C , 95% RH)		
	2.9	2.4	2.3	2.9	2.4	2.3
	3.5	2.5	2.0	2.2	2.2	2.2
	2.9	2.0	2.0	2.2	2.2	2.6
	3.1	2.1	2.3	2.4	2.4	2.0
	3.0	2.5	2.0	2.4	2.3	2.4
	3.0	1.9	1.8	2.0	2.5	2.6
	2.1	1.8	2.5	3.3	2.4	2.5
	2.4	1.8	2.5	3.2	2.5	2.6

the right side of the band which is later displaced to lower values of length as t approaches 10 days. For aging between 2 and 4 weeks, the ity curve moves again to higher values of pulled-out lengths of fibres. ly may exist for data corresponding to t = 0 which lie in the centre of the ead of to the right as we observe for the distribution of measurements of ond length. The Weibull constant m ranges between 1.6 and 2.5 (Table 1).

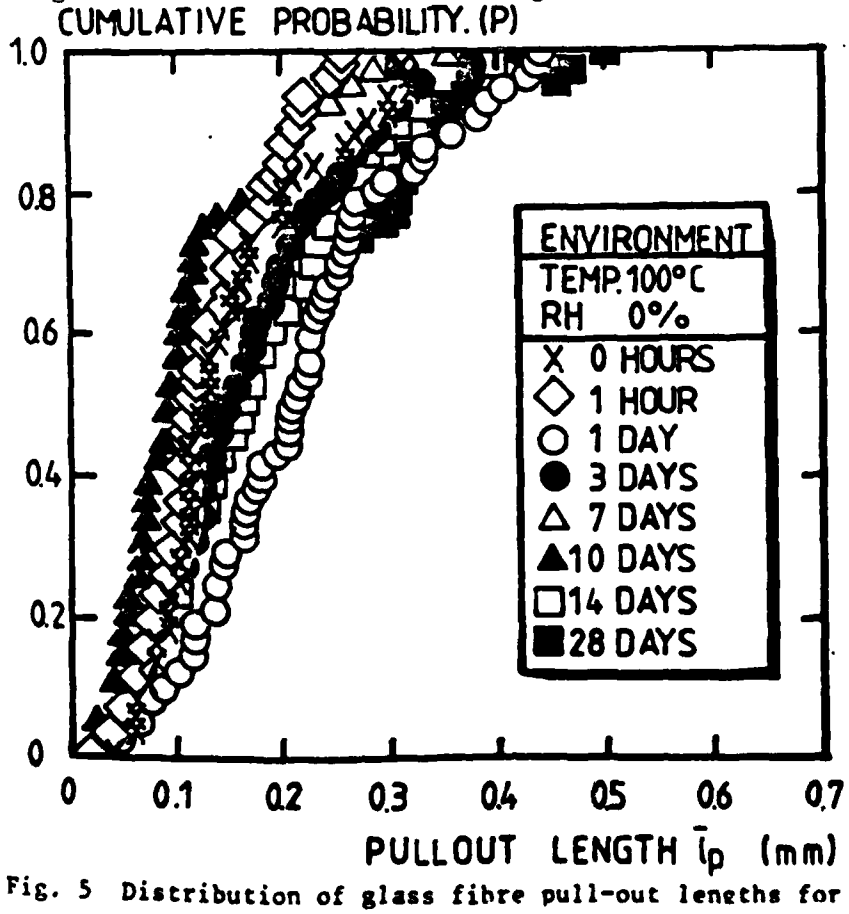

Fig. 5 Distribution of glass fibre pull-out lengths for

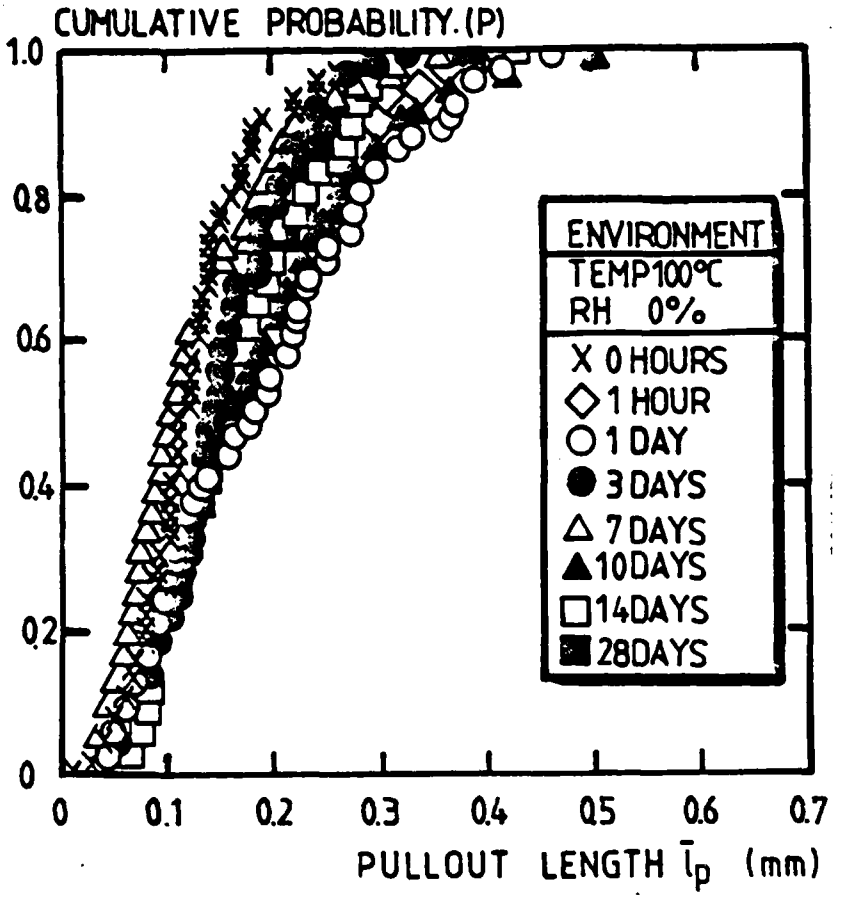

Fig. 6 Distribution of carbon fibre pull-out lengths for various aging times (100°C, 0% RH).

We do not observe any debonding of carbon fibres although the fibres do pull-out after snapping at flaws. The distribution of pull-out lengths fall in a narrow band with the superposition of data at low probabilities and separation of data at P = 1 (Fig. 6). The shortest pull-out lengths are observed at t = 0 and t = 7 days; the longest fibres are found at times of 1 day, 10 days and 14 days. Each movement of the distribution of data is consistent with observed variations in work of fracture as a function of time. The Weibull constant m lies between 1.8 and 2.5, similar to values corresponding to the pulling out of glass fibres (Table 1).

Cumulative probability diagrams displaying failure data of glass fibres and carbon fibres in epoxy aged at 100°C, 95% RH are shown in Figs. 7-9. Data essentially superimpose for exposure times up to 1 week and are located between distribution curves for t = 0 and t = 2-3 weeks. The data corresponding to t = 1 h and t = 10 days are between the distribution curves for 1 week and 2 weeks. The positions of the probability curves illustrate the time-dependence of the debonding process of glass fibres. At $t \leq 1$ h, the fibre debond length decreases; between 1 h and 3 days, the length increases; and between 3 days and 2 weeks, the length decreases once more. The maxima and minima in the work of fracture curve (Fig. 3) can be identified with these subtle movements of failure data. We see that m is between 2.0 and 2.4 and m = 3.3 for data collected in the first 10 days and following 2 weeks of aging, respectively (Table 1). The distribution of fibre pull-out data fall in narrow bands (Figs. 8, 9). Close inspection shows slight displacements of the probability curves to lower values of pull-out length with time to a similar extent that we observed data collected in a dry environment. The Weibull constant m is between 2.0 and 2.6 for both composite systems (Table 1).

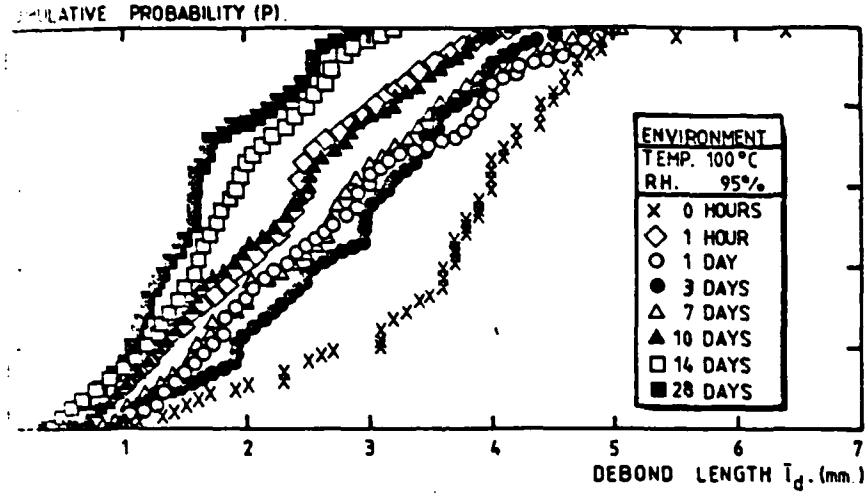

. 7 . Distribution of glass fibre debond lengths for various aging times (100°C, 95% RH).

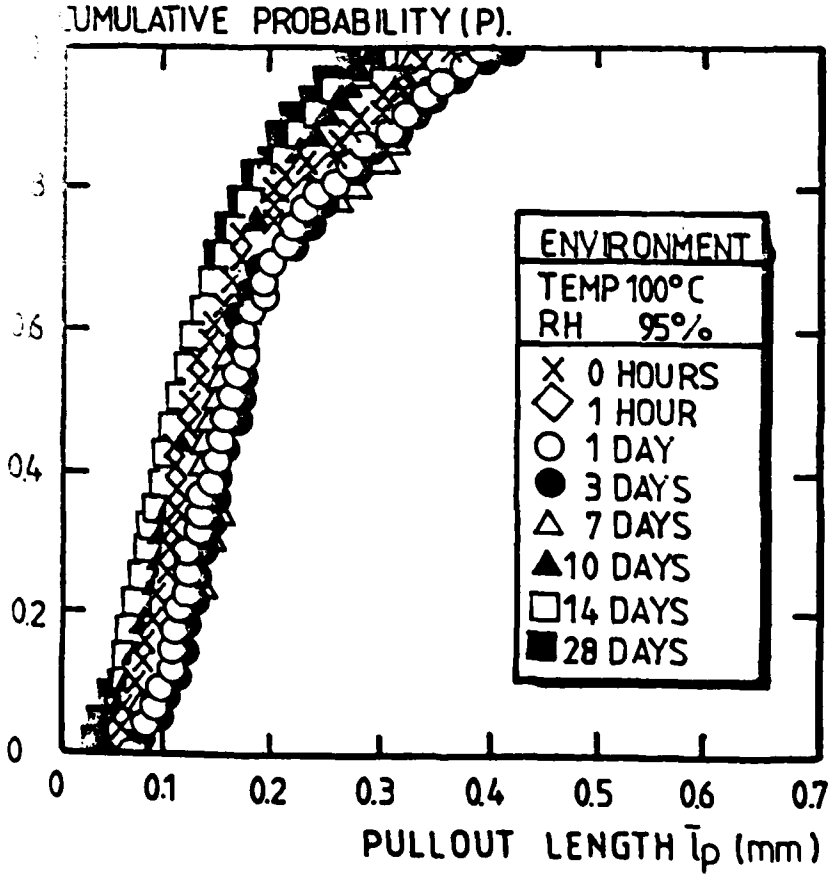

Fig. 8 Distribution of glass fibre pull-out lengths for various aging times (100°C, 95% RH).

MICROMECHANISMS OF FRACTURE

Models of the micromechanisms of crack extension to explain the origins of toughness in brittle fibrous composites have been proposed (Harris, Morley and Phillips, 1975) (Kirk, Munro and Beaumont, 1978). For the sake of brevity, we list three equations, based on physically sound models, to describe the energy dissipated in

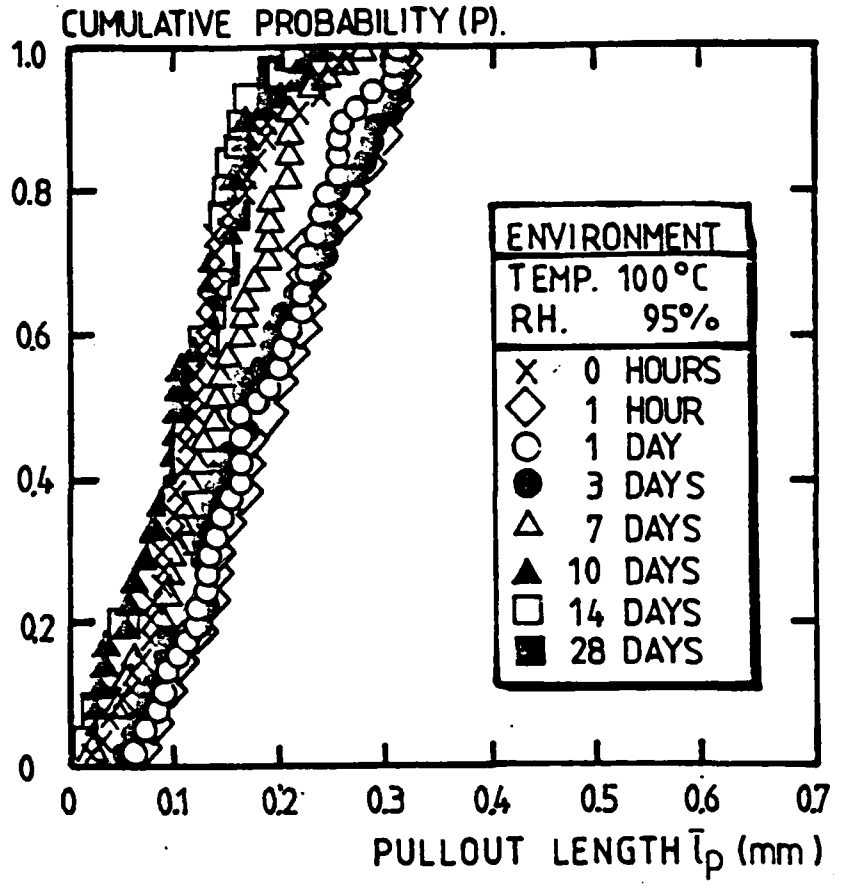

Fig. 9 Distribution of carbon fibre pull-out lengths for various aging times (100°C, 95% RH).

fracture. Figure 10 is a schematic illustration of the three mechanisms, involving debonding and extraction of fibres, together with equations. Equation (a) predicts the energy dissipated when a fibre under conditions of increasing load, slides with respect to the matrix over the unbonded portion of its length; equation (b) describes the release of stored elastic strain energy over the unbonded length of fibre when the fibre snaps; and equation (c) estimates the work done in extracting a broken fibre from its matrix socket against a frictional shear force. First, we calculate a characteristic fibre length for debonding and pulling out using eq. (5) for each aging cycle. We then use each equation in turn, together with the value of fibre debond length and fibre pull-out length to compute the three energy terms and total work to fracture the composite. The strength, Young's modulus and failure strain of the fibres are given below.[1] We estimate the frictional interfacial shear stress, τ, from a measurement of pull-out length by assuming that $\ell_p \propto \tau^{-1}$ (Kirk, Munro and Beaumont, 1978). The open symbols in Figs. 2, 3 are theoretical values of work of fracture based on the models and failure data. In all cases, there is excellent agreement between the experimental work of fracture and predicted fracture energy, although in general, theory overestimates the measurement of toughness.

---

[1] We have used for glass fibres $\sigma_f = 1.65$ GN/m^2; $E_f = 70$ GN/m^2; $\varepsilon_f = 0.01$; and for carbon fibres $\sigma_f = 2.4$ GN/m^2 and $E_f = 240$ GN/m^2.

THERMAL AND MOISTURE EFFECTS

Similarity between the work of fracture data and predicted values of fracture energy suggests that it is the energy dissipated during extraction of broken carbon fibres behind the tip of a crack that is the origin of toughness of carbon fibres in epoxy. The dissipation of energy during slippage of unbonded glass fibres close to a crack tip, and their subsequent extraction behind an advancing crack front can be equated to the work to fracture glass fibres in epoxy. In both systems, the fall in toughness with time at 100°C, 0% RH can be attributed to an improvement in bond strength. This can occur as a result of additional post-curing of the resin and contraction around the fibre. Such an "aging effect" manifests itself in a reduction in debond length of glass fibres, and a slight decrease in pull-out length of glass fibres and carbon fibres. These observations explain the larger reduction in toughness of the glass fibre composite.

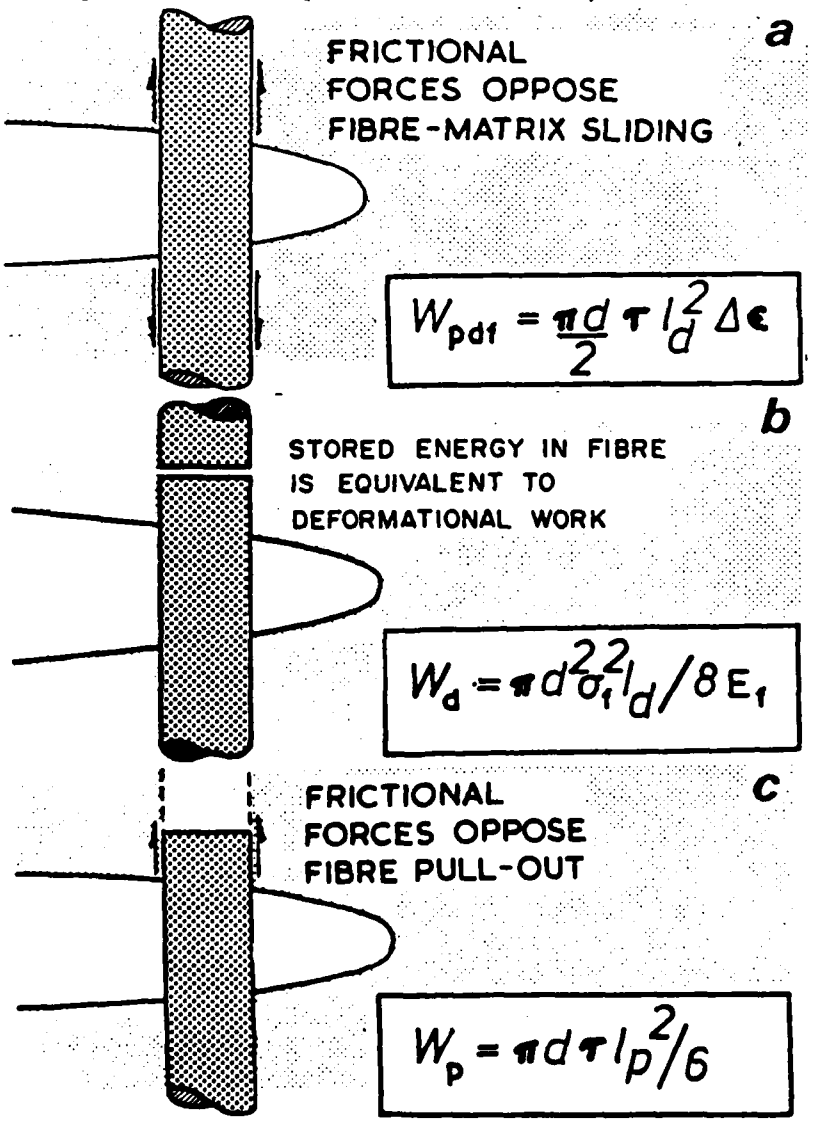

Fig. 10 Three micromechanisms of fracture:
(a) post-debond fibre sliding
(b) fibre fracture
(c) fibre pull-out.

The origin of the increase in toughness of glass fibres in epoxy after aging for 2 weeks at 100°C, 0% RH is unclear. We observe an increase in length over which the fibre debonds and a change in value of m, with little change in pull-out length. The inference is that the interfacial shear strength has decreased, perhaps due to degradation of the interface by some means. It may be that the chemical bond between glass fibre and matrix is weakened as a result of polymerisation of the silane coupling agent on the surface of the fibre (Ishida and Koenig, 1979).

A fall in work of fracture of both composite systems aged at 100°C, 95% RH for $t > 3$ days corresponds to a shift of fibre debond length and fibre pull-out length data to the left of the probability diagram, i.e., to shorter lengths. This may be attributed to an enhancement of interfacial shear strength as a result of moisture absorption and matrix swelling and an increase in radial compressive force of the matrix onto the fibres. We see from the fibre pull-out model, that an increase in bond strength reduces the fibre pull-out length and pull-out energy, as we observe. The collection of failure data and their relative positions to one another in the probability diagram support this hypothesis for $t > 3$ days.

The precipitous fall in work of fracture of the glass fibre composites at $t \leq 1$ h at 100°C, 0% RH corresponds to positional changes of the probability curves of failure data to lower values. The effect is also observed after annealing in the humid environment. Because of the short time involved, we believe that the effect is a thermal one. It may be that a moist surface of the fibres before impregnation with resin is drying out, an effect which is more pronounced in air at 0% RH. Alternatively, the short annealing treatment may cause relaxation of any residual stress in the matrix which affects the bond strength. Whatever the reason, the two composite systems behave differently at $t \leq 1$ h and the nature of the phenomenon is unknown to us at this time.

ACKNOWLEDGEMENTS

We wish to acknowledge the support of the Science Research Council under contract number ER/A 6537, and the Air Force Office of Scientific Research, Washington, D.C., under grant number AFOSR-78-3644. The gift of fibres from Mr L.N. Phillips of The Royal Aircraft Establishment, Farnborough, is gratefully received. We wish to acknowledge important discussions and comments by J. Wells.

REFERENCES

Beaumont, P.W.R., and Anstice, P.D. (1980). To be published in J. Mater. Sci.
Harris, B., Morley, J., and Phillips, D.C. (1975). J. Mater. Sci., 10, 2050.
Ishida, H., and Koenig, J.L. (1979). J. Poly. Sci., 17, 615.
Kirk, J.N., Munro, M., and Beaumont, P.W.R. (1978). J. Mater. Sci., 13, 2197.
Munro, M., and Beaumont, P.W.R. (1979). 3rd International Conference on Mechanical Behaviour of Materials, 3, 253. Edited by K.J. Miller and R.F. Smith and published by Pergamon Press (U.K.).

UNCLASSIFIED

SECURITY CLASSIFICATION OF THIS PAGE (When Data Entered)

REPORT DOCUMENTATION PAGE	READ INSTRUCTIONS BEFORE COMPLETING FORM
1. REPORT NUMBER: AFOSR-TR-80-1244	2. GOVT ACCESSION NO.: AD-A093 767	3. RECIPIENT'S CATALOG NUMBER
4. TITLE (and Subtitle): Hygrothermal Effects on the Micromechanisms of Crack Extension in Glass Fibre and Carbon Fibre Composites.	5. TYPE OF REPORT & PERIOD COVERED: FINAL rept.
	6. PERFORMING ORG. REPORT NUMBER
7. AUTHOR(s): PAUL D. ANSTICE, PETER W.R. BEAUMONT	8. CONTRACT OR GRANT NUMBER(s): AFOSR-78-3644
9. PERFORMING ORGANIZATION NAME AND ADDRESS: CAMBRIDGE UNIVERSITY/DEPART OF ENGINEERING, TRUMPINGTON STREET, CAMBRIDGE ENGLAND	10. PROGRAM ELEMENT, PROJECT, TASK AREA & WORK UNIT NUMBERS: 61102F, 2307/B2
11. CONTROLLING OFFICE NAME AND ADDRESS: AIR FORCE OFFICE OF SCIENTIFIC RESEARCH, BOLLING AFB DC 20332	12. REPORT DATE: 1980
	13. NUMBER OF PAGES: 11
14. MONITORING AGENCY NAME & ADDRESS (if different from Controlling Office): CUED/C-MAT/TR.75-1980	15. SECURITY CLASS. (of this report): UNCLASSIFIED
	15a. DECLASSIFICATION/DOWNGRADING SCHEDULE

16. DISTRIBUTION STATEMENT (of this Report)

APPROVED FOR PUBLIC RELEASE; DISTRIBUTION UNLIMITED

17. DISTRIBUTION STATEMENT (of the abstract entered in Block 20, if different from Report)

18. SUPPLEMENTARY NOTES

19. KEY WORDS (Continue on reverse side if necessary and identify by block number)

MICROMECHANISMS OF FRACTURE, GLASS FIBRES, CARBON FIBRES, HYGROTHERMAL EFFECTS, FAILURE ANALYSIS, PROBABILTY OF FAILURE

20. ABSTRACT (Continue on reverse side if necessary and identify by block number)

Hygrothermal aging effects and the micromechanisms of crack extension in glass fibre and carbon fibre composites are described. A new collection of failure data based on direct observation of fibres debonding, breaking and pulling out of a cracked epoxy matrix is presented. The data are summarized in cumulative probability diagrams which provide a convenient means for the comparison of fracture behavior of composite systems. These diagrams also demonstrate the effects of changes in environment and time in a given experiment in a manner useful for the failure analysis of a (over)

DD FORM 1 JAN 73 1473 EDITION OF 1 NOV 65 IS OBSOLETE

UNCLASSIFIED 400082

SECURITY CLASSIFICATION OF THIS PAGE (When Data Entered)

fibrous composite.